Pergamon

Acta Materialia 50 (2002) 565–574

Acta MATERIALIA

www.elsevier.com/locate/actamat

Imaging of the crystal structure of silicon nitride at 0.8 Ångström resolution[1]

A. Ziegler [a], C. Kisielowski [b], R.O. Ritchie [a,*]

[a] *Materials Sciences Division, Lawrence Berkeley National Laboratory, and Department of Materials Science and Engineering, University of California, Berkeley, CA 94720, USA*

[b] *National Center for Electron Microscopy, Lawrence Berkeley National Laboratory, Berkeley, CA 94720, USA*

Received 5 September 2001; received in revised form 21 September 2001; accepted 21 September 2001

Abstract

High-resolution transmission electron microscopy is utilized to examine the crystal structure of a silicon nitride ceramic using focus variation methods to achieve sub-ångström resolution at the absolute theoretical information limit of the transmission electron microscope. Specifically, crucial requirements of high instrumental stability, a coherent electron source and optimum imaging conditions have been met by the one-Ångstrom microscope (OÅM) at the National Center for Electron Microscopy in order to obtain a resolution of 0.8 Å. The resulting high-resolution images reveal the individual atom positions of the in-plane projected crystal structure of silicon nitride and permit detailed structural information. The images correspond closely to computed and simulated images of this crystal structure. © 2002 Acta Materialia Inc. Published by Elsevier Science Ltd. All rights reserved.

Keywords: Atomic-resolution transmission electron microscopy; Crystal structure; Ceramics

1. Introduction

In materials science, to comprehend the formation and interaction of defects, interfaces, nanostructures, etc., and their effect on the physical, mechanical and electrical behavior, information at the atomic level is clearly pertinent. Among the characterization techniques used to retrieve such information, high-resolution transmission electron microscopy (HRTEM) is the most utilized technique as it has the great advantage that it can interrogate structural information in two dimensions. However, to access truly atomic level information, the imaging instrumentation has to be in perfect alignment and highly stable, with an absolute minimum in high-voltage, lens-current and thermal-energy spread.

Recent progress with HRTEM, however, has made it possible to obtain sub-ångström resolution in a "mid-voltage" microscope via phase retrieval through focus variation, i.e., to extend the resolution well beyond its Scherzer point-to-point resol-

* Corresponding author. Tel.: +1-510-486-5798; fax: +1-510-486-4881.

E-mail address: roritchie@lbl.gov (R.O. Ritchie).

[1] Work supported by the Director, Office of Science, Office of Basic Energy Sciences, Materials Sciences Division of the US Department of Energy under Contract No. DE-AC03-76SF00098.

PII: S1359-6454(01)00363-9

ution of 1.7 Å to an expected information limit of about 0.8 Å [1]. The one-Ångstrom microscope (OÅM) at the National Center for Electron Microscopy (Lawrence Berkeley National Laboratory) has been used to demonstrate such resolutions at 0.89 Å and 0.85 Å [2–5], representing the highest resolution feasible with the present HRTEM design. The procedure utilized in this work is based on several such studies [6–17] and exploits the sub-ångström information limit of a field emission TEM in a particular manner via digital image processing [18,19] to produce electron exit waves limited only by the information limit of the HRTEM. Usually, a single HRTEM image represents a highly encoded mixture of the properties of the sample with those of the TEM. A reconstruction of the electron exit wave from a focused series of lattice images, on the other hand, allows the elimination of imaging artifacts, the extension of the resolution to the information limit and the simplification of image interpretation.

In this paper, we use this specific technique to image, for the first time, the crystal structure of a structural ceramic, namely silicon nitride, with an unprecedented resolution of 0.8 Å and a sensitivity that allows for the detection of single nitrogen columns.

2. Background

Bulk silicon nitride (Si_3N_4) ceramics have been investigated extensively over the last two decades, largely because their mechanical and physical properties are relevant for many high-temperature applications; these include high strength, high decomposition temperature (1900°C), good oxidation resistance, low coefficient of friction, negligible creep, good thermal shock properties, and good resistance to corrosive environments. In addition, thin silicon nitride films and coatings have been studied in order to understand electrical and thermal conductivity properties. All of these properties, and the processing and sintering behavior, rely on the specific crystal structure, the local chemistry, and the local bonding at interfaces. However, it has been challenging to assess this information experimentally because truly atomic level imaging on such ceramic structures has not been feasible.

The crystal structure data of the Si_3N_4 matrix, calculated using X-ray diffraction methods, have been used for computational modeling. However, confirmation of the computed bonding characteristics using direct imaging of the crystal structure and the structure of the interfacial regions with high-resolution transmission electron microscopy, specifically to identify the positions of the additive ions, has not been achieved at truly atomic resolution. A problem here is that a point-to-point resolution that reaches the theoretical information limit of the TEM of about 0.8 Å is required in order to identify single atom columns in the Si_3N_4 matrix in [0001] projection. Consequently, the focus variation technique provides the only means to date to obtain images at such a resolution.

3. Experimental procedures

3.1. Material

In this study, we examine a silicon nitride fabricated by Geyer and Hoffmann with newly developed two-step sintering technique, consisting of a dilatometer-controlled gas-pressure-sintering process and a successive hot-isostatic pressing densification [20]. Such highly pure and controlled processing was utilized to permit almost impurity-free densification without the usual glass encapsulation technique.

Si_3N_4 powder (UBE SN E10; Ube Industries, Yamaguchi, Japan) was sintered with 2 wt% Y_2O_3 (fine grade, HCST) to achieve a microstructure consisting of two morphologies of β-Si_3N_4 grains: predominantly acicular-shaped, with an average length of 5 μm and an aspect ratio of 8:1, and equiaxed, with a size of 0.5–1.5 μm. Samples for examination in the TEM were prepared by grinding, dimpling, and ion milling. The low-voltage ion milling was performed with a LINDA ion mill (Technoorg LINDA, IV3H/L ion beam thinning unit, Scientific Technical Development Ltd., USA) to produce foils with a thickness of less than 100 Å and with highly smooth surfaces, surface roughness $\leq$10 Å.

3.2. Electron microscopy

3.2.1. Electron microscope

Electron microscopy was performed with the NCEM OÅM, a Philips CM300/FEG/UT microscope modified to improve its information limit from the standard 1.05 Å [21] to 0.8 Å [2–5]. This 300 kV microscope is equipped with a field emission electron source and an ultra-twin objective lens of low spherical aberrations (C_s = 0.60 mm) and chromatic aberrations (C_c = 1.3 mm). With this microscope, lattice images can be recorded aberration free to a smallest distance of about 0.8 Å.

The specimen stage is a Philips double-tilt low-background holder with a tilting range of ±30°/±30°. Images are recorded digitally through an attached Gatan Image Filter (GIF) on a 2048×2048 pixel CCD (charge-coupled device) camera that allows for a total magnification up to 38 Mx. Electron exit waves were reconstructed from series of twenty lattice images using the Philips/Brite-Euram software developed by Coene and Thust [18,19].

3.2.2. Phase retrieval and image reconstruction

To understand the phase retrieval and image reconstruction technique, it is necessary to note that an exit-wave function emanating from the back plane of the specimen can be written as a function containing an amplitude and phase relationship:

$$\psi(r) = A(\boldsymbol{r})\cdot\exp(-i\phi_t(\boldsymbol{r})), \quad (1)$$

where $A(\boldsymbol{r})$ is the amplitude and $\phi_t(\boldsymbol{r})$ is the phase, which depends on the specimen thickness. However, the intensity I captured on the image plane is expressed as:

$$I = \psi\cdot\psi^* = |\psi|^2, \quad (2)$$

which is why phase information is lost. The successive projection of the electron exit wave into an image plane can be written as:

$$\Phi(\boldsymbol{u}) = H(\boldsymbol{u})\cdot\Psi(\boldsymbol{u}), \quad (3)$$

where $\boldsymbol{u}$ is the reciprocal-lattice vector representing the spatial frequencies, and $\Phi(\boldsymbol{u})$ and $\Psi(\boldsymbol{u})$ are the image and specimen function, respectively. $H(\boldsymbol{u})$ is the contrast transfer function (CTF) that describes how contrast is transferred into the image plane. This transfer function $H(\boldsymbol{u})$ characterizes microscope parameters such as the spherical aberrations C_s of the objective lens and the defocus Δf.

Spatial frequencies are related to the reciprocal of distance and therefore high spatial frequencies simply correspond to small distances. Hence high-resolution work requires high spatial frequencies. The CTF describes how these spatial frequencies (or contrast) are transferred from the specimen to the image in a TEM. A typical plot of the CTF for the classical optimum Scherzer defocus conditions, $\Delta f = -42$ nm, in a weak phase approximation is shown in Fig. 1. Two types of resolution can be defined, (i) the structural resolution limit and (ii) the theoretical information limit. The first crossover point determines the width of the passband for spatial frequencies to be transferred (from $\boldsymbol{u} = 0$ to $\boldsymbol{u}_{\text{crossover}}$), which in turn determines the structural resolution limit. The value of $\boldsymbol{u}_{\text{crossover}}$

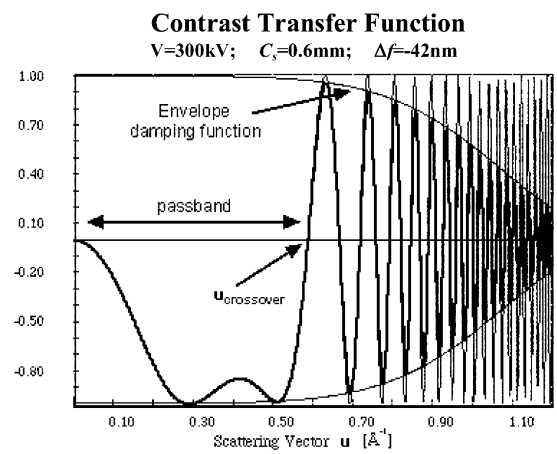

Fig. 1. A typical plot of the CTF for the classical optimum Scherzer defocus conditions, $\Delta f = -42$ nm, is shown. The value of $\boldsymbol{u}_{\text{crossover}}$ denotes the smallest distance ($\boldsymbol{u} = 1/\rho$) that can be resolved in the image, i.e., the structural resolution limit. Structural resolutions of about 1.7 Å can be achieved with a good microscope at intermediate voltages (300–400 kV). The observation that the amplitude of the CTF function decreases and vanishes at high spatial frequencies is due to the fact that the microscope is incapable of imaging the finest detail for those parameters (C_s, λ, Δf). A point of interest is where the signal becomes comparable to the noise; this occurs towards the end of the CTF plot at high spatial frequencies and is called the theoretical information limit.

denotes the smallest distance ($\boldsymbol{u} = 1/\boldsymbol{\rho}$) that can be resolved in the image. It is equally important to recognize here that the first crossover under Scherzer imaging condition:

$$\rho_s = 0.65 \cdot C_s^{1/4} \cdot \lambda^{3/4} = 1.7 \text{ Å}, \quad (4)$$

which defines the point-to-point resolution, is by a factor of approximately two larger than the microscopes information limit of about 0.8 Å. Structural resolutions of about 1.7Å can be achieved with a good microscope at intermediate voltages (300–400 kV).

The observation that the amplitude of the CTF function decreases and vanishes at high spatial frequencies is due to the fact that the microscope is incapable of imaging the finest detail for those parameters (C_s, λ, Δf). Reasons for this behavior are other than the simple information transfer characteristics. A finite spatial and temporal coherence act to damp the contrast transfer function and impose a limit as to which information can be transferred. This general envelope damping function imposed on the CTF defines the other type of resolution, the theoretical information limit. The point of interest is where the signal becomes comparable to the noise; this occurs towards the end of the CTF plot at high spatial frequencies and is called the theoretical information limit.

Phase reconstruction aims at the information contained between the structural resolution and the theoretical information limit. It is pertinent that the oscillatory behavior of the CTF function is "well-behaved". Plotting in Fig. 2 the CTF for a defocus value of (a) $\Delta f = -137$ nm and (b) $\Delta f = -350$ nm shows that the structural resolution decreases and the passband moves towards higher spatial frequencies as the defocus decreases. The envelope function does not decay as fast as in the case of the Scherzer defocus and it extends further out. The oscillations of the CTF extend to higher spatial frequencies under the envelope function. The "well-behaved" manner of the oscillations extends beyond the 1 Å mark. This behavior can be described mathematically and used for the reconstruction of the phase information. If an image is taken under this underfocus condition, its structural resolution might be very low, but it contains a significant amount of phase information

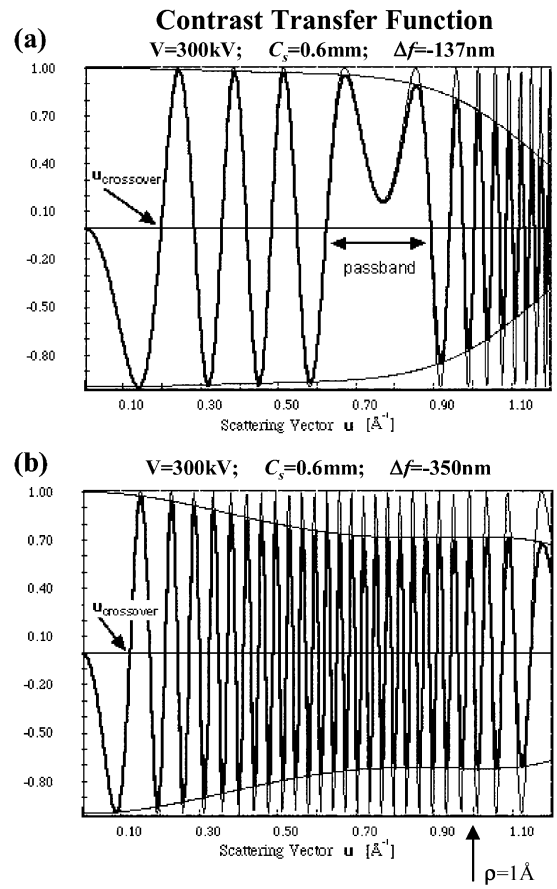

Fig. 2. Plotting the CTF for a defocus value of (a) $\Delta f = -137$ nm and (b) $\Delta f = -350$ nm shows that the structural resolution decreases and the passband moves towards higher spatial frequencies as the defocus decreases. The envelope function does not decay as fast as in the case of the Scherzer defocus and it extends further out. The oscillations of the CTF extend to higher spatial frequencies under the envelope function. The "well-behaved" manner of the oscillations extends beyond the 1 Å mark. This behavior can be described mathematically and be used for the reconstruction of the phase information.

hidden in the rapid but "well-behaved" phase changes of the CTF function. The spatial frequencies that contribute to the image need to be unscrambled and organized according to their position in the CTF, that is, according to their sign, amplitude and phase. The phase retrieval procedure restores the proper amplitudes and phases of the electron exit waves down to the microscopes information limit and removes undesired effects of delocalization.

It can be seen that the choice of a large underfocus aids the information transfer at spatial frequencies close to the theoretical information limit. This was typically extracted from 20 lattice images recorded around an underfocus of −260 nm with a constant defocus interval of ~2.4 nm for successive lattice images.

3.3. Computer simulations

Corresponding computer simulations of the crystal structure were conducted using the commercial program CrystalKit [22]. The HRTEM image simulations were subsequently performed using these structure models as input to the commercial program MacTempas [23]. Through-focus and through-thickness image simulations can be created with this program from the model crystal structures. MacTempas is based on the multislice method, whereby the structure model is sliced perpendicular to the direction of the incident beam. The potential content of each single slice modifies the incoming electron wave, which is then projected onto the next slice and propagated through the entire structure model [23].

4. Results and discussion

4.1. Crystal structure of silicon nitride

Fig. 3(a) shows the experimentally reconstructed phase of the electron exit wave from the crystal structure of β-Si_3N_4 projected along the [0001] direction. It reveals all details of the modeled structure of β-Si_3N_4 that is shown in schematic form in Fig. 3(b). The larger scattering power of silicon compared with nitrogen makes the silicon columns appear as brighter spots. Indeed, the hexagonal crystal structure can be directly copied into the experimental image of Fig. 3(a). Simulations of the electron exit wave confirm this assignment [inset in Fig. 3(a)]. Two nitrogen positions are visible in this projection. The first one is clearly separated among three silicon columns and the second one appears as a shoulder on the silicon columns. A line scan across phase maxima [Fig. 3(c)] reveals their presence. However, the nitrogen signal is weak at this thickness. Therefore, it is not fully separated from the silicon signal. The Fourier components of transformed lattice images extend into the sub-ångström region [Fig. 3(d)]. Thus, the phase image of Fig. 3(a) displays sub-ångström resolution close to the 0.8 Å information limit of the microscope. Experimentally, sample tilt is a most limiting factor to obtain such high quality images.

The reconstruction process provides for easier image interpretation. Fig. 4 shows a comparison of the regular lattice image obtained under regular Scherzer defocus conditions [Fig. 4(b)] with the corresponding reconstructed phase image of the electron exit wave [Fig. 4(a)]. It is apparent that the Scherzer image displays interference spots at locations where no atom columns are present in the real crystal lattice. Since lattice images are interference patterns, their appearance changes with defocus and sample thickness. This is demonstrated in Fig. 5 where an array of simulated lattice images is presented; in this array, the sample thickness is increased from top to bottom and the defocus value increased from right to left. It is apparent that the appearance of the image changes drastically with focus and thickness. In contrast, the phase of the reconstructed electron exit wave does not change with focus; it exhibits intensity maxima at the positions of the atomic columns. Chemical information can be accessed through the magnitude of the phase change if the thickness can be estimated. In this regard, the image simulations can be used to ascertain the thickness of the sampling area in the specimen by comparing, for example, the Scherzer defocus image in Fig. 4(b) with the array of simulated images in Fig. 5. Using this approach, we find that the sample thickness to be approx. 80–90 Å in this case.

Salient criteria have to be met for such Scherzer and phase-reconstructed HRTEM imaging; these include the presence of atoms, specimen thickness and electron oscillation in the specimen.

For imaging, it is the atom column density oriented in the direction of the incident electron beam that is important; a denser column of ions causes stronger scattering of the incident electrons. For phase-reconstructed imaging, a conflict can arise when the column density is low. Specifically, if the bonding characteristics are such that atomic dis-

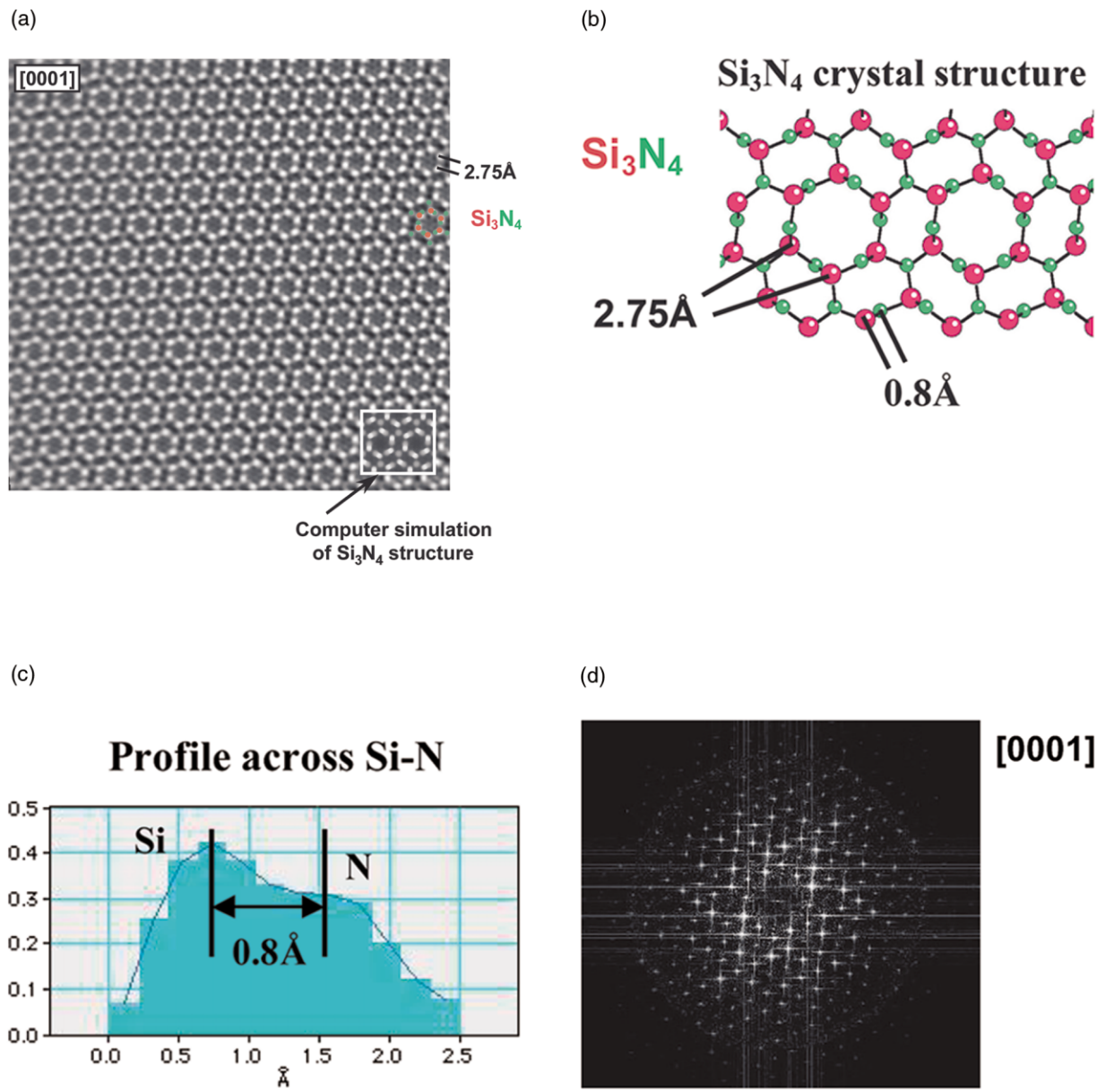

Fig. 3. Reconstructed image showing the crystal structure of silicon nitride (a). The insert shows a computer simulation of the crystal structure where it can be seen how well the simulation matches with the phase reconstructed image. The computer simulation was performed using the model shown in (b), displayed as the in-plane projected image of the crystal structure of silicon nitride displaying the interatomic distances. A line scan taken across the phase maxima of a close Si–N pair in the phase reconstructed image reveals the resolution of this imaging technique, 0.8 Å (c). The Fourier components of transformed lattice images extend into the sub-ångström region (d).

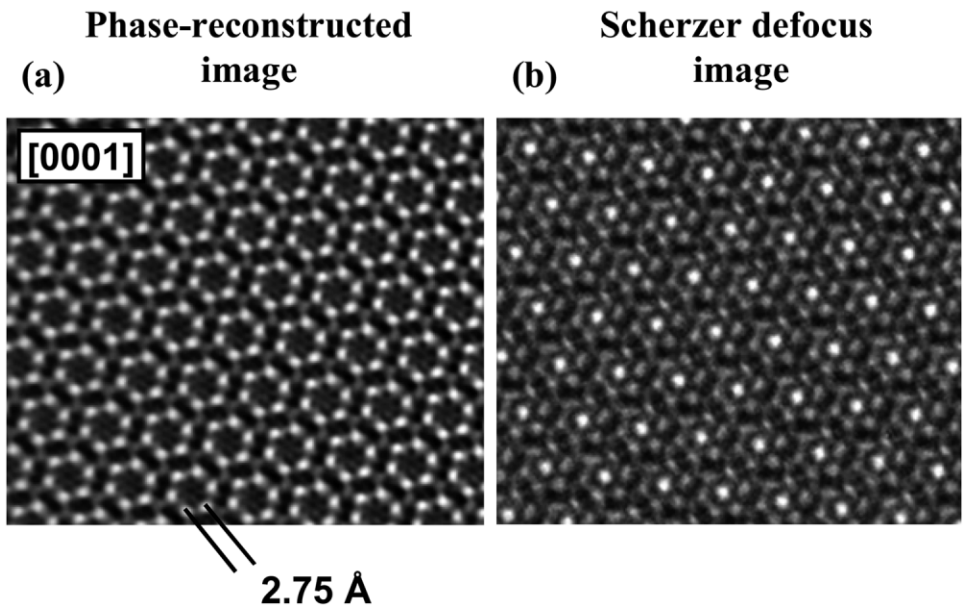

Fig. 4. The phase reconstructed image (a) is compared to the Scherzer defocus image (b) where it can be seen that the single image as represented in the Scherzer defocus condition does not contain as much information as the phase reconstructed image. Indeed, the Scherzer image displays bright spots at locations where there are no atoms in the real lattice, in particular in the middle of the Si-hexagon. A single HRTEM image represents a highly encoded mixture of the properties of the object with those belonging to the TEM. Phase retrieval and focal-series image-reconstruction allows eliminating imaging artifacts, which complicate the interpretation of single images. The phase reconstruction technique utilizes the information of twenty images recorded under different defocus values.

tances are large along the columns, this necessitates using a thicker sample to exceed a minimum atom density for good imaging contrast; however, foils thicker than 100 Å are not optimal for phase reconstruction purposes.

The interaction of electron waves with material in zone axis orientation is strongly dynamic. Amplitudes and phases of the electron wave oscillate with the sample thickness and this oscillation period is called extinction distance ξ. Lighter atoms produce a longer extinction distance compared to heavier atoms. Relevant extinction distances were extracted from ref. [24] for the present elements; they are: ξ(Si)~256 Å, ξ(N)~304 Å. Maximum image contrast and thus atom visibility at the exit plane occur when the specimen thickness coincides with half an extinction oscillation. Image contrast vanishes at a full extinction oscillation (Fig. 6). The thickness of the current specimen results in almost full image contrast for both types of atoms.

The crisp and detailed images obtained with focus-variation, image-reconstruction, and sub-Ångstrom HRTEM imaging are promising for further investigations of the actual structure of silicon nitride, in particular to examine interfaces and grain boundaries in this material. For example, sintering additive ions are known to segregate to such boundaries, which often consist of nanoscale amorphous intercrystalline films. These films profoundly affect the mechanical properties of ceramics at both ambient and elevated temperatures. The control of their structure and chemistry is thus critical to developing new and improved ceramic microstructures with superior structural performance; indeed, current studies are directed at using focus-variation methods to relate the strength, toughness and fatigue properties of Si_3N_4 ceramics

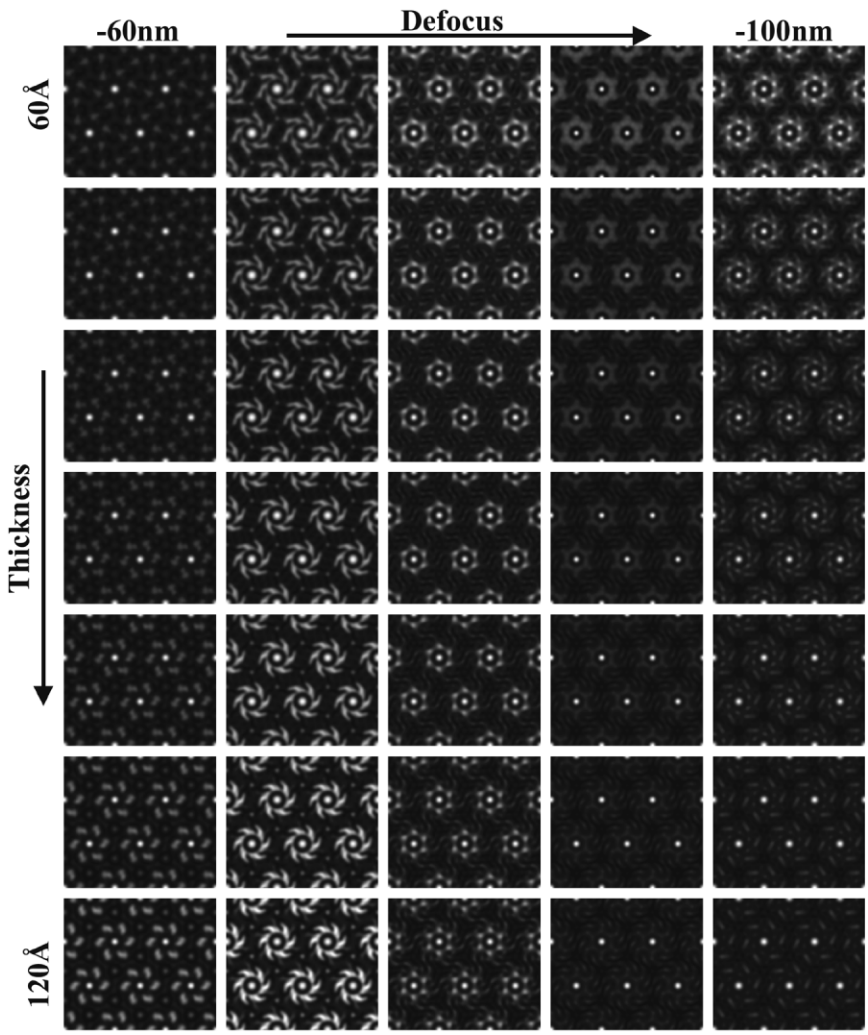

Fig. 5. An array of simulated images is shown as they would appear in the TEM for different imaging conditions. The thickness increases from top to bottom and the defocus value decreases from left to right. The differences in defocus and thickness are not very large but it can be clearly seen that every image is different. Note for example how small changes in defocus cause significant changes in the image. Small variations make one perceive a different picture of the object under investigation. Every image contains a different set of phase information, all belonging to the same area of interest. The phase retrieval and image reconstruction method allows for these individual sets of information to be combined into one image, obtaining a much more complete picture of the object. The image simulations can also be used to ascertain the thickness of the sampling area in the real specimen.

to such a HRTEM characterization of the grain boundary films [25].

5. Conclusions

Focus-variation image-reconstruction HRTEM imaging has been successfully demonstrated for investigating the atomic structure of a ceramic material with an unprecedented resolution. Specifically, the crystal structure of silicon nitride has been imaged for the first time at a resolution of 0.8 Å, i.e., at the theoretical information limit of a HRTEM. The resulting high-resolution images reveal the individual atom positions of the in-plane projected crystal structure and allow retrieving

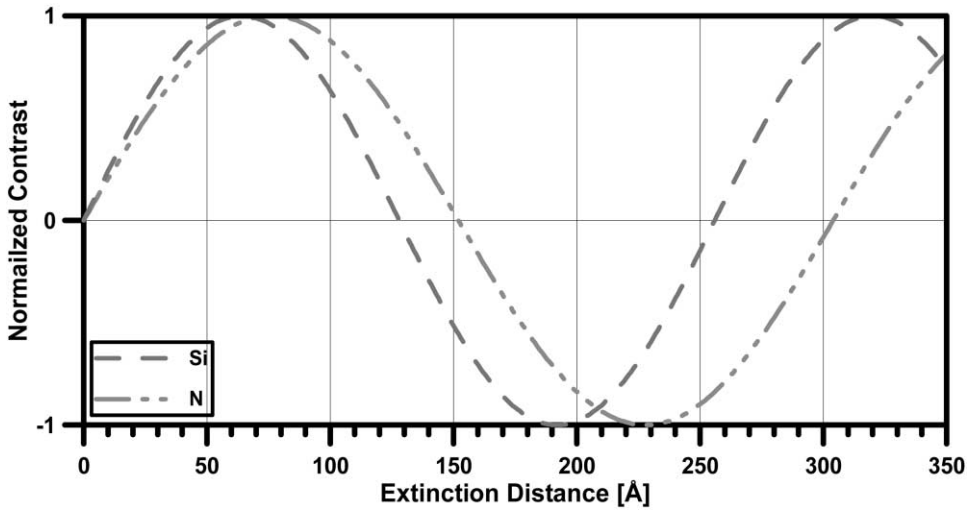

Fig. 6. Electron scattering is very dynamical and the propagating electron wave exhibits a specific wavelength—an extinction distance ξ—that depends on the scattering power of a specific column of atoms. Lighter atoms produce a longer extinction distance compared to heavier atoms. The approximate specific extinction distances extracted from ref. [25] for the present elements are: ξ(Si)~256 Å, ξ(N)~304 Å. Maximum image contrast and thus atom visibility at the exit plane occur when the specimen thickness coincides with half an extinction oscillation. Image contrast vanishes at a full extinction oscillation.

very detailed structural information. In fact, such sensitivity allows for the detection of single nitrogen columns. The images agree well with computed and simulated images of the corresponding silicon nitride crystal structure.

Acknowledgements

This work was supported by the Director, Office of Science, Office of Basic Energy Sciences, Materials Sciences Division of the US Department of Energy under Contract No. DE-AC03-76SF00098. The authors wish to thank Dr. M.J. Hoffmann of the Universität Karlsruhe for processing the silicon nitride, Chris Nelson and Dr. Mike O'Keefe of the National Center for Electron Microscopy, for assistance with the HRTEM, and Dr. Rowland M. Cannon for helpful discussions.

References

[1] Van Dyck D, Lichte H, Van der Mast KD. Ultramicroscopy 1996;64:1.
[2] Kisielowski C, Nelson EC, Song C, Kilaas R, Thust A. Microscopy and Microanalysis 2000;6:6.
[3] O'Keefe MA, Hetherington CJD, Wang YC, Nelson EC, Turner JH, Kisielowski C, Malm JO, Mueller R, Ringnalda J, Pan M, Thust A. Ultramicroscopy 2001;89:215.
[4] Wang YC, Fitzgerald A, Nelson EC, Song C, O'Keefe MA, Kisielowski C. Microscopy and Microanalysis 1999;5:822.
[5] Kisielowski C, Hetherington CJD, Wang YC, Kilaas R, O'Keefe MA, Thust A. Ultramicroscopy 2001;89:243.
[6] Lichte H. Ultramicroscopy 1992;47:223.
[7] Van Dyck D, Op de Beeck M, Coene WMJ. Optik 1993;93:103.
[8] Coene WMJ, Janssen G, Op de Beeck M, Van Dyck D. Phys Rev Lett 1992;69:3743.
[9] Op de Beeck M, Van Dyck D, Coene WMJ. Ultramicroscopy 1996;64:167.
[10] Kirkland EJ. Ultramicroscopy 1984;15:151.
[11] Kirkland EJ. In: Proc 6th Pfefferkorn Conference on Image and Signal Processing in Electron Microscopy, Niagara Falls, Canada, 1988:139.
[12] Saxton WO. J Microsc Spectrosc Electron 1980;5:665.
[13] Op de Beeck M, Van Dyck D. Ultramicroscopy 1996;64:153.
[14] Buist AH, Van den Bos A, Miedema MAO. Ultramicroscopy 1996;64:137.
[15] Tang D, Zandbergen HW, Jansen J, Op de Beeck M, Van Dyck D. Ultramicroscopy 1996;64:265.
[16] Thust A, Overwijk MHF, Coene WMJ, Lentzen M. Ultramicroscopy 1996;64:249.

[17] O'Keefe MA. In: Krishbab K, editor. Microstructures of Materials, Berkeley (CA): San Francisco Press; 1993:121.
[18] Coene WMJ, Thust A, Op de Beeck M, Van Dyck D. Ultramicroscopy 1996;64:109.
[19] Thust A, Coene WMJ, Op de Beeck M, Van Dyck D. Ultramicroscopy 1996;64:211.
[20] Geyer A. PhD thesis, University of Karlsruhe, Karlsruhe, Germany, 1997.
[21] Bakker H, Bleeker A, Mull P. Ultramicroscopy 1996;64:17.
[22] The CrystalKit and MacTempas packages are both available from Total Resolution, National Center for Electron Microscopy, Lawrence Berkeley National Laboratory, Berkeley (California).
[23] Kilaas R. In: Bailey GW, editor. 45th Annual Proc of EMSA, Baltimore (MD): San Francisco Press; 1987:66.
[24] Van Dyck D, Chen JH. Solid State Commun 1999;109:501.
[25] Ziegler A, Kisielowski C, Hoffmann MJ, Ritchie RO. J Am Ceram Soc, in review.